International Journal of Mechanical, Industrial and Aerospace Sciences
ISSN: 2517-9950
Vol:4, No:12, 2010

Numerical Investigation of Flow Past Cylinder in Cross Flow

M. H. Alhajeri, Jasem Alrajhi, Mohsen Alardhi, Saleh Alhajeri

***Abstract*—**A numerical prediction of flow in a tube bank is reported. The flow regimes considered cover a wide range of Reynolds numbers, which range from 380 to 99000 and which are equivalent to a range of inlet velocities from very low (0.072 m/s) to very high (60 m/s). In this study, calculations were made using the standard k-e model with standard wall function. The drag coefficient, skin friction drag, pressure drag, and pressure distribution around a tube were investigated. As the velocity increased, the drag coefficient decreased until the velocity exceeded 45 m/s, after which it increased. Furthermore, the pressure drag and skin friction drag depend on the velocity.

***Keywords*—**Numerical - Fluid - Flow - Turbine - Cooling - Blade.

I. Introduction

IN spite of the simple geometry, numerical simulation of turbulent flow past a circular cylinder still remains a challenging problem for computational fluid dynamicists. Zdravkovich [1] reviewed the flow interference between two circular cylinders in various arrangements. An excellent review of experimental investigations for tube banks in cross flow was given in Zukauskas [2]. Jun et al. [3] and Fan et al. [4] used numerical methods to simulate fluid flow in a tube bank in cross flow, using particles suspended in a gas flow. Most recently, Wilson et al. [5] reviewed and studied laminar and turbulent flow over a single cylinder and across in-line and staggered tube banks. Lee and Daichin [6] and Akilli et al. [7] conducted experimental and numerical investigations of flows over cylinders. In this study, flow fields were investigated in single cylinder in cross flow.

II. Results and Discussion

The single, cylinder model or consists of a two-dimensional duct with a circular, cylinder in the middle. The model assumed to be two-dimensional because the depth of the channel is very small comparing to the channel length and width. The length of the duct was 0.5 m 25 times the cylinder diameter or 25d, and the width was 0.2 m or 10d, while the diameter of the cylinder is 0.02 m. The cylinder was placed in the middle of the x-distance and y-distance of the duct. The outlet is far beyond any recirculation zones that may be created by the cylinder. This is also to minimize the effects of the out-flow boundary conditions on the flow characteristics in the vicinity of the cylinder. The in-flow boundary is located at a distance of four cylinder diameters in front of the first cylinder. The mesh is unstructured and contains 9108 cells.

The inlet velocity in this model ranges from very low (0.072 m/s) to very high (60 m/s), and these velocities are equivalent to Reynolds numbers from 380 to 99000. Nishimura [8] and Zukauskas [2] reported that in the case of the flow past cylinder, the laminar flow regime is at Reynolds number less than 100. K-ε turbulence model is used here due to its capability in this wide range of turbulence model.

Turbulent flows in the regions close to the walls are affected by the presence of the walls. The mean velocity is affected by the no-slip boundary condition, and the fluctuating velocity is also changed by the presence of the wall. Since the walls are the main source of vorticity and turbulence, they could have significant impacts on the fidelity of numerical solutions. The very well-known standard wall function, which is based on the laws of the wall for mean velocity, was employed in this study. The outlet was set as pressure outlet where the code will calculate the values at the outlet according to the condition ahead of it. The fluid used in this investigation was air with a density of 1.2 Kg/m^3 and a viscosity of 1.4 x 10^{-5} kg/m-s.

In the grid independency study, three cases were enough to reach the sufficient grid size to continue the study. The first case is the coarse grid with grid size of 6372 cells. The second case has grid size of 9108 cells. The third case (the densest case) used grid size of 14156 cells

Three profiles were chosen to compare the three meshes. One profile was at 0.22 m from the inlet and located upstream from the cylinder; the second was at 0.28 m from the inlet and in the middle of the cylinder; and the third was 0.35 m from the inlet and downstream from the cylinder. The locations of the profiles were chosen carefully to show the separation and the circulation. Case A (coarse) differs in few points from the other cases whereas the fine and dense cases (cases B and C) have identical curves. The results do not depend on the grid in cases B and C, and case B (0.5 mesh and 3760 cells) was used in this study.

M. H. Alhajeri, Mechanical Power Engineering, Faculty of Technological Studies, PAAET,. P.O. Box 34000, Roudha, Kuwait 73460 (e-mail: mhhajeri@gmail.com).

Jasem Alrajhi, Automotive and Marine Engineering, Faculty of Technological Studies, PAAET,. P.O. Box 433 Alardiya, Kuwait (e-mail: ajasem@gmail.com)

Mohsen Alardhi, Automotive and Marine Engineering, Faculty of Technological Studies, PAAET, (e-mail: alardhi@ymail.com)

Saleh Alhajeri, Automotive and Marine Engineering, Faculty of Technological Studies, PAAET (e-mail:mhhajeri@gmail.com).

Flow past a single cylinder was investigated with six different inlet velocities of 0.68, 1, 15, 30, 45, and 60 m/s, covering the range of Reynolds numbers from 1100 to 99000. Figs 1 and 2 show the velocity magnitude profiles at the position where x is equal to 0.265 m in the channel length. The profile is just behind the cylinder or downstream from it, and this profile across the stagnation region was caused by the existence of the solid obstacle. The Figures show profiles for different inlet velocities of 0.68, 1, 15, 30, 45, and 60 m/s. The velocity increases just before and just after the stagnation region, because recirculation behind the cylinder acts like another obstacle just as the cylinder itself is an obstacle. This is why the velocity increases just before the recirculation or stagnation regions, and this is also made clear in the next figures for profiles crossing the cylinder. The velocity approaches zero in the middle of the profile, creating the recirculation region with the size of 20% of the channel width, which is larger than the cylinder diameter. The recirculation size increases as the inlet velocity (or Reynolds number) increases. As Reynolds number increases, the velocity in the center of the recirculation decreases.

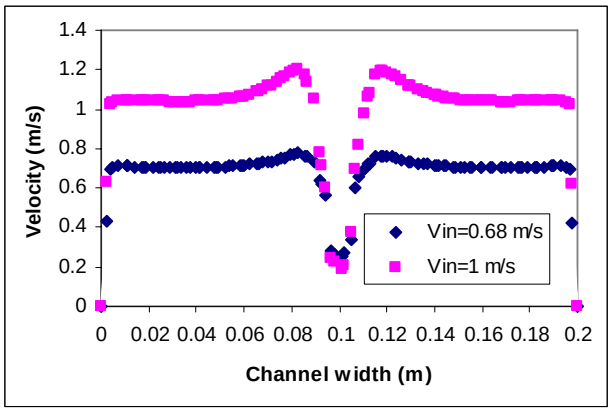

Fig. 1 Velocity magnitude profile at x = 0.265m behind the cylinder for low inlet velocities 0.68 and 1 m/s

The velocity increases a few cells from the cylinder, as shown in Figs. 3 and 4. In those figures, the velocity magnitude profiles at x = 0.25 m cross the middle of the cylinder. The increments in the velocity are high for the low Reynolds numbers, to about 80%, and they are low for high Reynolds numbers, reaching 42%. Due to law of wall, the velocity decreases to zero very close to the wall.

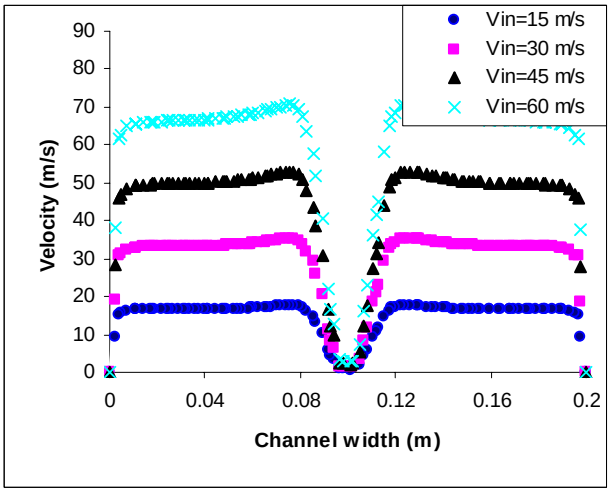

Fig. 2 Velocity magnitude profile at x = 0.265m behind the cylinder for high inlet velocities 15, 30, 45 and 60 m/s

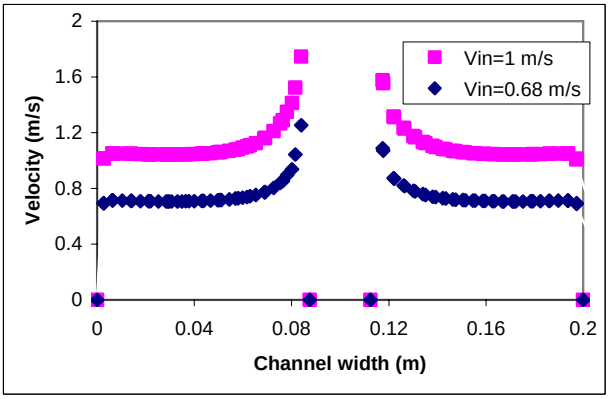

Fig. 3 Velocity magnitude profile at x = 0.25m behind the cylinder for low inlet velocities 0.68 and 1 m/s

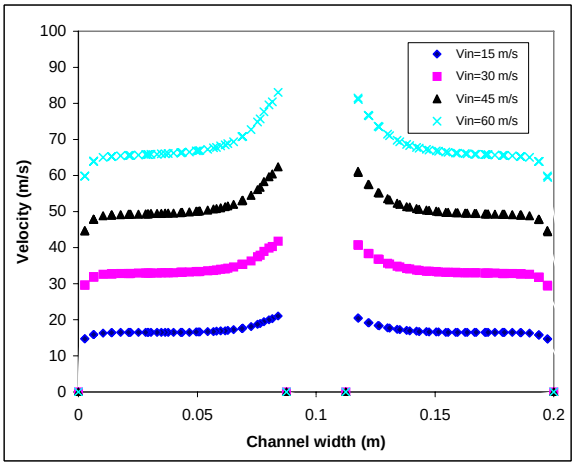

Fig. 4 Velocity magnitude profile at x = 0.25m behind the cylinder for high inlet velocities 15, 30, 45 and 60 m/s

The variations of drag coefficient with velocity are shown in Fig 5. As the velocity increases, the drag coefficient decreases

due to the existence of the square of velocity in the lower part of the C_d equation, however after the velocity exceeds 45 m/s, the drag coefficient starts to increase. At this point, it can be stated that the inlet velocity of 45 m/s is the optimum velocity in the case of a single cylinder. Fig 6 shows the pressure distribution around the cylinder for different inlet velocities. All the pressure distributions have the same trend, but they have different values. The maximum C_d value occurred at 0 degree or at the front of the cylinder. Here, the velocity is reduced to the minimum (almost zero) due to the blockage that resulted from the existence of the cylinder, while the minimum value of C_d occurred at an angle of 90°, where the velocity reached the lowest width that satisfies the continuity equation. Downstream from the cylinder, where the stagnation region is found, the value of C_d increases and becomes constant while crossing the large stagnation region. The pressure drag increased as the inlet velocity increased from 15 to 60 m/s in four steps. However, the pressure drag increased from 3.8 to 14 N as inlet velocity increased from 15 to 30 m/s, and, as it increased from 45 to 60 m/s, the pressure drag increased with a greater differential equal to 23 N, as shown in Fig 7. The same results for pressure drag were attained in Fig 8 for skin friction drag with inlet velocity. Figs 7 an 8 show that the inlet velocity is one of main factors that governs the changes in pressure drag and skin friction drag. The drag force is equal to the sum of skin friction drag and pressure drag.

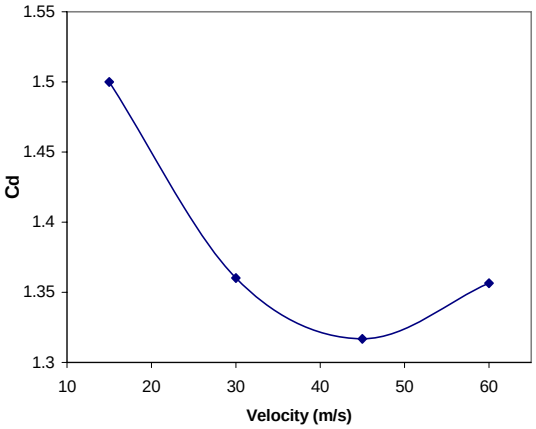

Fig. 5 Variation of drag coefficient (C_d) with Velocity

III. Conclusions

A computational fluid dynamics investigation of flow, drag past circular cylinder was conducted for a wide range of Reynolds numbers from 380 to 99000 and for the related range of inlet velocities that varied from very low (0.072 m/s) to very high (60 m/s). The velocities approach zero at the back of the cylindrical cylinder, creating eddies and a stagnation region that is larger than the cylinder diameter. The optimum drag coefficient was found at an inlet velocity of 45 m/s. Before the inlet velocity reached 45m/s, the drag coefficient increased as the inlet velocity decreased, while the opposite behaviour occurred when the inlet velocity exceeded the optimum. Furthermore, the maximum C_d value was found in the front of the cylinder, while the minimum C_d value was found at the sides of the cylinder. Almost linear behaviour was evident between the inlet velocity and the pressure drag or skin friction drag.

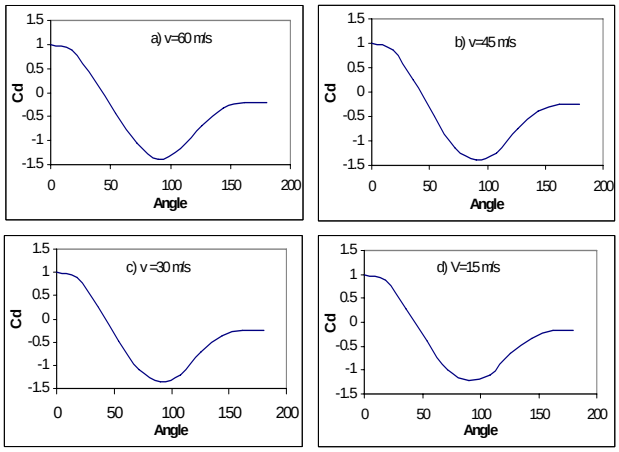

Fig. 6 Pressure distribution around a cylinder

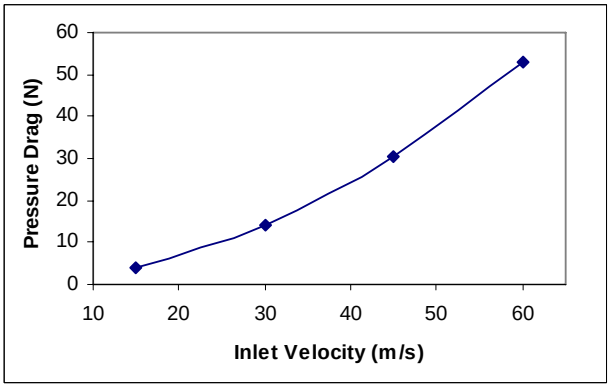

Fig. 7 Pressure drag for different inlet velocity

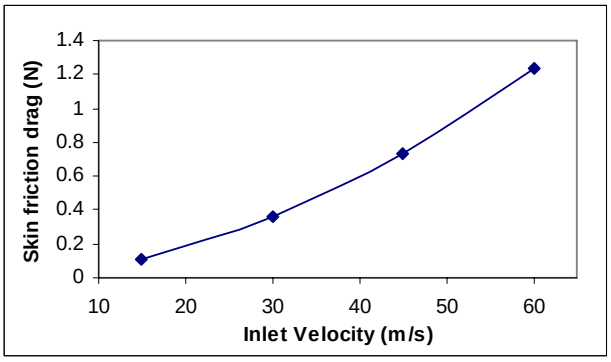

Fig. 8 Skin friction drag for different inlet velocity

REFERENCES

[1] M. Zdravkovich, "Review Of Flow Interference Between Two Circular Cylinders In Various Arrangements," Journal of Fluid Engineering 99 (1977) 618-633.
[2] A. Zukauskas, *Heat Transfer from Tubes in Cross-Flow*, Advances in Heat Transfer 8 (1972) 93-160.
[3] Y. Jun, and W. Tabakoff, *Numerical Simulation of A Dilute Particulate Flow (Laminar) Over Tube Banks*. Journal of Fluid Engineering 116 (1994) 750- 770
[4] J. Fan, Q. Zhou, Q. Hua, K. Cen, "Numerical computation of particle laden gas flows past staggered tube banks undergoing erosion Powder Technology 80 (1994) 1-10.
[5] S. Wilson, K. Bassiouny, "Modeling of Heat Transfer For Flow Across Tube Banks," *Chemical Engineering and Processing 39 (2000) 1-14*.
[6] S.J. Lee, A. Daichin, "Flow past a circular cylinder over a free surface: Interaction between the near wake and the free surface deformation," *Journal of Fluids and Structures 19 (2004) 1049–1059*.
[7] H. Akilli , A. Akar, C. Karakus, "Flow characteristics of circular cylinders arranged side-by-side in shallow water Flow Measurement and Instrumentation 15 (2004) 187–197.
[8] T. Nishimura, *Flow Across Tube Banks, Encyclopedia of Fluid Mechanics* Gulf publishing, 1 (1986) 763-785.